M2-Polarized Macrophages Mediate Wound Healing by Regulating Connective Tissue Growth Factor via AKT, ERK 1/2, and STAT 3 Signaling Pathways

Si-Min Zhang
Zhongshan Hospital Fudan University
Chuan-Yuan Wei
Zhongshan Hospital Fudan University
Qiang Wang
Zhongshan Hospital Fudan University
Lu Wang
Zhongshan Hospital Fudan University
Lu Lu
Zhongshan Hospital Fudan University
Fa-Zhi Qi (qifazhi@163.com)
Zhongshan Hospital Fudan University https://orcid.org/0000-0003-1442-275X

Research Article

Keywords: Wound healing, Macrophage, M2 polarization, Connective tissue growth factor, Fibrosis

Posted Date: June 22nd, 2021

DOI: https://doi.org/10.21203/rs.3.rs-624342/v1

Version of Record: A version of this preprint was published at Molecular Biology Reports on August 16th, 2021. See the published version at https://doi.org/10.1007/s11033-021-06646-w.

Abstract

Background: Timely and sufficient recruitment of M1 macrophages and M2 polarization are necessary for fibrous repair during cutaneous wound healing. The inherent mechanism of how M2 polarization mediate wound healing is worth exploring and illustrating. Abnormally up-regulated connective tissue growth factor (CTGF) is closely related with multiple organ fibrosis, including cardiac, pulmonary, hepatic, renal, and cutaneous fibrosis. Previous studies have reported that M2-polarized macrophages contribute to hepatic and renal fibrosis by secreting CTGF. It is worth discussing if M2 macrophages regulate fibrosis through secreting CTGF in cutaneous wound healing.

Methods: We established the murine full-thickness excisional wound model and inhibited macrophages during proliferation phase (mainly M2 and M1-M2 polarization) with clodronate liposomes to analyze how M2 macrophages mediate wound healing rates, collagen deposition, collagen 1/3 expression, and Ki67 expression in *vivo*. Furthermore, M2 polarization was induced by IL-4 and in *vitro*. $F4/80^{+}CD206^{+}$ M2 macrophages were measured by flow cytometry. The morphological characteristics were observed. Secretion of IL-6, TNF-α, IL-10, TGF-β1, and CTGF was tested by ELISA. *CTGF* gene of M2 was blocked using siCTGF. Effects of M2 on proliferation and migration of fibroblasts were detected by CCK8 and cellular wound healing assay. Protein level of AKT, ERK1/2, and STAT3 pathway were assessed by western blotting.

Results: Depletion of macrophages at proliferation phase (mainly M2 and M1-M2 polarization) resulted in delayed cutaneous wound closure and down-regulation of wound healing rates, collagen deposition, collagen 1/3 expression, and Ki67 expression. M2 polarization was induced, which producing more CTGF, TGF-β1, and IL-6, as well as less TNF-α and IL-10. Blockade of CTGF in M2 macrophages deactivated fibroblast proliferation and migration. Addition of recombinant CTGF restored the promotional effects of M2 macrophages on fibroblast proliferation and migration. Blockade of CTGF in M2 mediate fibroblasts via down-regulating AKT, ERK1/2, and STAT3 signaling pathway.

Conclusion: Our research, for the first time, indicated that M2-polarized macrophages promoted cutaneous wound healing by secreting CTGF, which further mediating proliferation and migration of fibroblasts via AKT, ERK1/2, and STAT3 signaling pathway.

1. Introduction

Fibrous repair generally happens after organ injury[1]. In plastic surgery, fibrous repair is related to pathological scars and chronic refractory wounds, including hypertrophic scar (HTS), keloid (K), as well as diabetic ulcers. There are also many other skin diseases associated with fibrogenic response, such as scleroderma, nephrogenic systemic fibrosis and skin fibrosis after radiotherapy[1]. In adults, fibrous repair contains two periods, including fibre deposition and fibre degradation. The first period, named fibre deposition, usually starts from the 4th or 5th day, remains active for about 1 week, and mitigates gradually. This period is paralleled with the inflammation phase and the tissue proliferation phase.

Collagen-rich matrix initially begins to accumulate from wound-edge to internal site of the granulation. The second period, named fibre degradation, mainly happened during the tissue remodeling phase. Fibrogenesis during wound healing is a dynamic and complex process, but the mechanism is not clear enough.

During wound healing, fibrous repair plays an important role. In adults, an inevitable result of tissue remodeling in wound healing is fibrosis and scarring[2]. However, in embryonic and foetal mice, the consequence is scarless healing. The differences might result from lacking infiltration of macrophages in E11.5, E12.5, E13.5 embryos. Later in E14.5 foetuses, macrophages are able to rapidly recruit to wound sites within 12 hours post injury[3]. Similarly in adults, macrophages invade toward excisional wounds within 6 hours[4]. However in PU.1 null mice, which is characterized by “macrophageless”, wound repair appears scar-free as in embryos[5]. These researches reveal that early macrophages recruitment plays a central role in wound healing, determining fibrous repair and scar formation.

Macrophages recruit to wound site mainly from peripheral blood soon after the wound occurs. Large amounts of M1 macrophages infiltrate in the wound area at 1 to 2 days post injury[6]. M1 macrophages further polarized to M2 macrophages at 3 days post injury[7]. The timely and sufficient polarization of “pro-inflammatory” M1 to “anti-inflammatory” M2 macrophages is necessary for wound healing. Blockade of M1-M2 polarization is found to be closely related to delayed wound healing[8]. In diabetic wound healing, there are excessive M1 macrophages and inadequate M2 macrophages. Oppositively, hypertrophic scar and keloid are overloaded with M2 macrophages[9]. Thus, M1 phenotype and M2 phenotype produce different effects in cutaneous wound healing.

Connective tissue growth factor (CTGF), also known as CCN2, is a secretory polypeptide belonging to CCN family. CCN family is composed of three serum-induced immediate-early genes, containing *CTGF*, Cysteine-rich 61 gene (*CYR61)*, and Nephroblastoma over-expressed gene (*NOV*) [10, 11]. Till now, abnormally up-regulated CTGF has been tested in multiple organ fibrosis, including cardiac, pulmonary, hepatic, and renal fibrosis[12–15]. In several cutaneous fibrosis, CTGF has also been suggested to exert pro-fibrotic effects[16–18]. In murine full-thickness excisional wound model as well as human burn injuries, CTGF accumulated at the wound site from 0 to 7 days post injury[19]. It has been reported that exogenous CTGF facilitated fibrosis in diabetic wound healing[16, 20, 21]. Elevated level of CTGF was defined in systemic sclerosis; however, inhibition of CTGF sharply reduced cutaneous fibrosis[16, 20, 21, 22].

Previous studies have showed that CTGF can not only be secreted by human umbilical vein endothelial cells (HUVEC) and fibroblasts, but also be produced by M2 macrophages[22, 23]. CTGF secreted by M2 macrophages has been reported to contribute to hepatic and renal fibrosis. In hepatic fibrosis during human schistosomiasis, M2 macrophages activated quiescent hepatic stellate cells (qHSC) to activated HSC (aHSC) through secreting transforming growth factor-beta1 (TGF-beta 1), vascular endothelial growth factor (VEGF), and CTGF. Moreover, TGF-beta 1 promoted aHSC proliferation via heat shock protein 47. Differently, VEGF and CTGF directly stimulate aHSC proliferation, leading to collagen

deposition, fibrosis, cirrhosis, even carcinoma in liver schistosomiasis[24]. In renal fibrosis during immunoglobulin A nephropathy (IgAN), high expressions of CTGF in M2 macrophages were responsible for glomerular collagen 1 deposition, matrix expansion, and glomerular/interstitial fibrosis[25]. In chronic allodraft nephropathy (CAN), M2 macrophages, which were identified with high secretion of pro-fibrotic factors (TGF-beta 1, CTGF, and fibroblast growth factor 2), might promote interstitial fibrosis progression[26]. Nevertheless, it is not clear if M2 macrophages promote fibrosis through secreting CTGF in wound healing.

In this research, we hypothesized that macrophages exerted essential functions in cutaneous excisional wounds. Macrophages promoted cutaneous wound healing with the help of increased proliferation and fibrosis. Fibrous repair would be mainly dominated by M2 macrophages, but not M1 phenotype. Potential mechanism was further assessed. Our study disclosed the role of M2 macrophages in wound healing, providing new potential targets for promoting healing process.

2. Materials And Methods

2.1 Animals

C57BL/6 mice, provided by Shanghai Laboratory Animals Center, aged 6-8w, weighted 20-25g, were applied in this research. Male mice, which were specific pathogen-free, were housed individually in cages and bred. Our manipulations were supported by the Ethics Committee of Zhongshan Hospital Fudan University.

2.2 Animal model and experimental groups

Before modeling, mice were firstly intraperitoneal (i.p.) injected with 1% pentobarbital sodium at a dose of 50 mg/kg body weight. The dorsal skin were prepared by shaving with electronic razor and sterilized with 75% ethanol. A 6 mm full-thickness excisional wound was produced each mouse.

We randomly divided mice into two groups: (1) Control group (PBS): mice (n = 5) accepted an i.p. injection of 200 μL 1×PBS at 4-day post injury and 100 μL 1×PBS at 6- and 8-day post injury. The skin tissues were obtained at 9-day post injury and fixed in 4% paraformaldehyde solution for 24 hours. (2) Macrophage depletion group (Clodronate liposome): mice (n = 5) received an i.p. injection of 200 μL clodronate liposomes (FormuMax Scientific Inc., CA, USA) at 4-day post surgery and 100 μL clodronate liposomes at 6- and 8-day post injury. The skin tissues were obtained at 9-day post injury and fixed in 4% paraformaldehyde solution for 24 hours.

2.3 Measuement of wound healing rates

The wound were taken photos at 0-, 5-, 7-, and 9-day post injury. The areas of wounds were assessed by ImageJ software. The wound healing rates were measured by ([original wound area]-[wound area])/[original wound area]×100%.

2.4 Masson’s trichrome staining

At 9-day post injury, the wound tissues were obtained by scissors and fixed using 4% paraformaldehyde. After dehydration, the wound tissues were soaked in dimethylbenzene. After embedding in parraffin, the wound tissues were sectioned (3 μm/slice). Masson's trichrome staining was further performed. The collagen volume fraction (CVF) was determined at 200× magnification and based on the volume ratio of collagen (stained blue) area in total area.

2.5 Immunstaining

At 9-day post injury, the wound tissues were obtained. Collagen 1 and collagen 3 were assessed by immunohistochemistry (IHC). Briefly, 3 μm parraffin-embedded slices of the wound tissues were dewaxed and hydrated. To block endogenous peroxidase, the slices were embedded in fresh 3% hydrogen peroxide (H_2O_2) at 37℃ for 30 minutes. Antigen retrieval was then completed by microwave oven with citric acid buffer (0.01 M). After cooling, the slices were incubated in blocking reagent (#P0102, Beyotime, Shanghai, China) at regular temperature (RT) for 1 hour. The slices were incubated with collagen 1 (#NB600-408, NOVUS Biologics, 1:250 dilution) and collagen 3 in dilution of 1:250 (#PA5-27828, invitrogen) overnight at 4℃. After washing, the slices were treated with secondary antibody (Jackson ImmunoResearch Laboratories, 1:200 dilution). The slices were successively stained with diaminobenzidine and hematoxylin. After dehydration, the slices were transparented with dimethylbenzene and coated with neutral balsam. Five different and random visual fields were photoed under optical microscope. The mean densities of collagen 1 and collagen 3 were estimated by Image-Pro Plus 6.0 software.

At 9-day post injury, the wound tissues were obtained. $CD206^+$ M2 macrophages were detected by immunofluorescence (IF). To measure proliferation, $Ki67^+$ cells in the wound tissues were marked by IF staining. After rewarming to RT, 5 μm optimal cutting temperature compound (OCT)-embedded frozen sections of the wound tissues were incubated in blocking reagent (#P0102, Beyotime, Shanghai, China) at RT for 1 hour. The sections were incubated with CD206 (#ab64693, Abcam, 1:500 dilution) and Ki67 (#9129, Cell Signaling Technology, 1:400 dilution) overnight at 4℃. The sections were washed and incubated with anti-goat (for CD206) and anti-rabbit (for Ki67) secondary antibody in dilution of 1:200 (Jackson ImmunoResearch Laboratories). The sections were further stained with DAPI and finally coated with anti-fade mounting medium (#0100-01, SouthernBiotech). Five different and random visual fields were photoed under fluorescent microscope. The amounts of CD206 and Ki67 were detected by ImageJ.

2.6 Cell lines and cell culture

RAW264.7 (mouse macrophages) cell line and L929 (mouse fibroblasts), which were purchased from the Cell Bank of the Chinese Academy of Sciences (Shanghai, China), were harvested in incomplete Roswell Park Memorial Institute (RPMI) 1640 medium (KeyGen BioTECH, China) supplemented with 10% fetal bovine serum (#S711-001S, LONSERA, Uruguay) in the presence of 5% CO2 at 37℃.

Treatment of unstimulated RAW264.7 (M0 macrophages) with interleukin-4 (IL-4) (#214 – 14, PeproTech, USA) was applied as a method for M2 macrophage polarization by incubation of RAW264.7 with 20

ng/mL IL-4 in 37℃/5% CO2 for 24 hours.

2.7 Confirmation of M2 macrophage polarization by flow cytometry

1×10^6 unstimulated RAW264.7 macrophages (non-IL-4 group) and IL-4-stimulated RAW264.7 macrophages (IL-4 group) were collected and washed with flow cytometry staining buffer. After centrifugation at 1500×g for 5 minutes, two groups of macrophages were dyed with PE rat anti-mouse F4/80 (eFluor 570, #41-4801-80, invitrogen, 1:50 dilution) at 4℃in the dark for least 30 minutes. After washing with flow cytometry staining buffer and centrifugation, macrophages were dealt with reagent A of fixation & permeabilization kit (#70-GAS003, MULTI SCIENCES (LIANKE) BIOTECH, China) at RT in the dark for 15 minutes. After centrifugation, macrophages were incubated with rabbit anti-mouse CD206 (Alexa Fluor® 488, #ab195191, Abcam, USA), which was diluted in reagent B of fixation & permeabilization kit. After washing and centrifugation, macrophages were resuspended in flow cytometry staining buffer and filtered with 70 μm cellular filter before testing. Macrophages were examined using a flow cytometer (BD FACSCanto Ⅱ, BD Biosciences). Percentages of $F4/80^+CD206^+$ M2 macrophages were analyzed in FlowJo V10 software.

2.8 Morphological characteristics of M2 macrophage polarization

After IL-4 stimulation, unstimulated RAW264.7 in non-IL-4 group (M0 macrophages) and IL-4-stimulated RAW264.7 in IL-4 group (M2 macrophages) were observed under optical microscope. Representative morphological characteristics of macrophages in two groups were observed at 200× magnification.

2.9 Detection of pro-fibrotic and anti-fibrotic factors by elisa

IL-10, TGF-β1, CTGF, IL-6, and TNF-α secreted by unstimulated RAW264.7 in non-IL-4 group (M0 macrophages) and IL-4-stimulated RAW264.7 in IL-4 group (M2 macrophages) were detected by Elisa kit (Kingmorn, China). To further examine the inhibitory efficiency of siCTGF in M2 macrophages, secreted protein levels of CTGF in control siRNA group and siCTGF group were assessed by elisa.

Fresh FBS-free cellular supernatants of two groups were collected at 24 h and 48 h. To remove impurities and granules, supernatants were centrifugated at 3000 rpm for 10 minutes. The microelisa stripe plates were recovered to RT in the dark for 20 minutes. Six standard samples (50 μL/well) were set at 0, 125, 250, 500, 1000, and 2000 pg/mL. 10 μL supernatants of two groups and 40 μL diluent were added to each well with three repetitions. Samples in each well were incubated with 100 μL HRP-conjugated antibody at 37℃ in the dark for 1 h. After washing with 1×wash buffer for three times, the plates were incubated with a mix substrate of 50 μL reagent A + 50 μL reagent B at 37℃ in the dark for 15 minutes. After incubation with 50 μL stop solution per well, OD values were assessed by Epoch2 microplate reader (BioTek Instruments, Inc., Winooski, VT, USA).

2.10 Blockade of CTGF by siCTGF

To analyze if M2 macrophages regulate L929 via secreting CTGF, M2 macrophages were dealt with siCTGF. Three kinds of siCTGFs were designed and synthesized by Genomeditech (Shanghai, China). SiCTGF 1: 5'-CUAUGAUGCGAGCCAACUG-3', 3'-CAGUUGGCUCGCAUCAUAG-5'; siCTGF 2: 5'-CGCAAGAUCGGAGUGUGCA-3', 3'-UGCACACUCCGAUCUUGCG-5'; siCTGF 3: 5'-GGGACAAUGACAUCUUUGA-3', 3'-UCAAAGAUGUCAUUGUCCC-5'. Briefly, M2 macrophages were seeded into 24-well plates (2×10^5 cells/well) and cultured with 1640 + 10%FBS medium in the presence of 5% CO2 at 37°C. Macrophages were utilized for further research at 80% confluence. SiCTGF was diluted with Opti-MEM. Lipofectamine^{TM}2000, diluted with Opti-MEM, stewed at RT for 5 minutes. A mixture of diluted siCTGF and diluted lipofectamine^{TM}2000 was created at RT for 18–20 minutes. Macrophages were dealt with the mixture (100 μL/well). After 6 h, medium was replaced with fresh complete medium. Inhibitory efficiency of siCTGF were examined by western blotting (intracellular protein level) and elisa (secreted protein level).

2.11 Cell proliferation by CCK8 assay

To determine different effects of M0 and M2 macrophages on L929 (fibroblasts) proliferation, FBS-free supernatants of macrophages (24 h) were applied on L929. Cell proliferation of L929 was assessed at 0, 24, and 48 h using CCK8 assay. Briefly, L929 (fibroblasts) were seeded in 96-well plates (1000 cells/well) and cultured with 1640 + 10%FBS medium at 37°C/5% CO2 for 24 h. After cell attachment, each well was replaced with 10 μL CCK8 + 90 μL FBS-free 1640 medium. Reaction of CCK8 was performed at 37°C/5% CO2 for 1.5 h. The values of OD were measured at 450 nm using Epoch2 microplate reader (BioTek Instruments, Inc., Winooski, VT, USA), representing cell proliferation at 0 h. After washing with 1×PBS for three times, free-PBS supernatants of M0 macrophages (non-IL-4 group) and M2 macrophages (IL-4 group) at 24 h were added to L929. As same as detection at 0 h, cell proliferation of L929 at 24 h and 48 h was assessed by CCK8 assay.

To analyze if M2 macrophages regulate L929 proliferation via secreting CTGF, M2 macrophages were dealt with siCTGF. FBS-free supernatants of M2 macrophages (24 h) in control siRNA group and siCTGF group were applied on L929. Cell proliferation of L929 was assessed at 0, 24, and 48 h using CCK8 assay as described above.

For further confirmation, recombinant CTGF was applied on fibroblasts along with FBS-free conditioned medium of M2 macrophages. Three groups were included: control siRNA group, siCTGF group, and siCTGF + CTGF group. The terminal concentration of CTGF was 2.0 μg/mL. Cell proliferation of L929 was assessed at 0, 24, and 48 h using CCK8 assay as described above.

2.12 Cell migration by wound healing assay

To determine different effects of M0 and M2 macrophages on L929 (fibroblasts) migration, FBS-free supernatants of macrophages (24 h) were applied on L929. Cell migration of L929 was assessed at 0, 24, 48, and 96 h using wound healing assay. Briefly, L929 (fibroblasts) were seeded into 6-well plates (2×10^5 cells/well) and cultured with 1640 + 10%FBS medium in the presence of 5% CO2 at 37°C for 6–8 hours. After cell attachment, the crossed straight scratches were induced by the tip of 200 μL pipette. To remove

cell debris, L929 fibroblasts were washed with uncompleted 1640 medium for three times. Fibroblasts were added with FBS-free supernatants of unstimulated RAW264.7 (M0 macrophages) and stimulated RAW264.7 (M2 macrophages), and then cultured in 5% CO_2 at 37℃. The wound areas were photoed at 0, 24, 48, and 96 h. The wound closure rates were analyzed.

To analyze if M2 macrophages regulate L929 migration via secreting CTGF, M2 macrophages were dealt with siCTGF. FBS-free supernatants of M2 macrophages (24 h) in control siRNA group and siCTGF group were applied on L929. Cell migration of L929 was assessed at 0, 24, and 48 h as described above.

For further confirmation, recombinant CTGF was applied on fibroblasts along with FBS-free conditioned medium of M2 macrophages. Three groups were included: control siRNA group, siCTGF group, and siCTGF + CTGF group. The terminal concentration of CTGF was 2.0 μg/mL. Cell migration of L929 was assessed as described above.

2.13 Western blotting

To determine different effects of M0 and M2 macrophages on AKT/STAT3 signaling pathway and ERK1/2/STAT3 signaling pathway in L929 (fibroblasts), FBS-free supernatants of macrophages (24 h) were applied on L929. After 48 h induction, total protein levels of AKT, ERK1/2, STAT3 as well as phosphorylation level of AKT, ERK1/2, and STAT3 were assessed by western blotting.

Briefly, L929 fibroblasts were washed with 1×PBS after treatment with FBS-free supernatants of macrophages for 24 h. Fibroblasts were collected with 1×PBS and centrifuged at 1000 rpm for 5 min. The sedimentation of fibroblasts in the bottom of 1.5 mL centrifuge tube was further treated with 100 μL lysis buffer on the ice for 30 minutes. Next, fibroblasts were centrifuged at 12000×g for 15 minutes. The supernatants were collected. The protein concentrations of supernatants were assessed by bicin-choninic acid (BCA) assay. A volume of 20 μL 5×loading buffer was added for protein denaturation.

Extracted proteins were initially separated on 10% sodium dodecyl sulfate-polyacrylamide gel electrophoresis (SDS-PAGE) at 100 V. After separation, proteins were transferred onto the nitrocellulose membrane (NCM) at 0.20 A. After 2 hours, the NCM was blocked in QuickBlock™ western block buffer (#P0252-500ml, Beyotime, China) at RT. After 15 minutes, the NCM was incubated with primary antibodies overnight at 4℃. Primary antibodies included: AKT (#4691, Cell Signaling Technology, USA, 1:1000 dilution), p-AKT (Ser473, #4060, Cell Signaling Technology, USA, 1:2000 dilution), ERK1/2 (#4695, Cell Signaling Technology, USA, 1:1000 dilution), p-ERK1/2 (Thr202/Tyr404, #9101, Cell Signaling Technology, USA, 1:1000 dilution), STAT3 (#9139, Cell Signaling Technology, USA, 1:1000 dilution), p-STAT3 (Tyr705, #9145, Cell Signaling Technology, USA, 1:2000 dilution), and GAPDH (#60004-1-Ig, proteintech, USA, 1:5000 dilution). After washing with 1×TBST, the NCM was further incubated with secondary antibodies at RT. After 1 hour, the NCM was washed with 1×TBST three times. Finally, protein bands were displayed using BeyoECL Star kit (#P0018AS, Beyotime, China). Relative band densities were analyzed by ImageJ software.

2.14 Statistical Analysis

All of the data were expressed as means ± standard deviation (SD). Evaluation of differences between groups were addressed by one-way ANOVA test and unpaired *t* test using GraphPad Prism 7. Differences were considered statistically significant when $P<0.05$.

3. Results

3.1 Macrophages are associated with fibrosis during cutaneous wound healing

In order to evaluate how macrophages influence wound healing, we created a murine wound model as previously described[27]. As shown in Fig. 1, the wound was established at 0-day post injury. Macrophages were depleted with clodronate liposome at 4-, 6-, and 8-day post injury. The wound healing rates were estimated according to the wound photos at 0-, 5-, 7-, and 9-day post injury. The wound tissues were collected at 9-day post injury and stained for markers of collagen, macrophages, and proliferation in Fig. 2. The wound healing delayed as a result of macrophage depletion (Fig. 2A). Depletion of macrophages led to remarkable reduction of wound healing rates at 5-, 7-, and 9-day post injury compared with those in control group (Fig. 2B). Differences were statistically significant ($P<0.01$).

3.2 Clodronate liposome effectively depleted macrophages

During the 9-day observation, the macrophage depletion group of mice received clodronate liposome (or PBS as control) at 4-, 6-, and 8-day post injury. The wound tissues at 9-day post injury were assessed for macrophages. M2 macrophages, the profibrotic phenotype, were stained by immunofluorescence of CD206. Control group exhibited extensive M2 macrophage infiltration in wound tissues, which was markedly attenuated following macrophage depletion (Fig. 2I). As shown in Fig. 2J, the number of $CD206^+$ M2 macrophages significantly declined from (283 ± 39) to (112 ± 41). A significant difference in M2 number was observed in clodronate group and control group ($P<0.01$).

3.3 Macrophages promoted collagen deposition during wound contraction

As the main component of extracellular matrix, collagen fibers deposite in granulation during wound healing. Polymetric and monometric collagen fibers are highlighted by masson's trichrome staining. The wound tissues were stained for collagen 1 and collagen 3, representative collagen components in the wound site.

The wound tissues depleted of macrophages during wound healing were assessed for collagen components. The wound tissues were revealed by masson's trichrome staining. Following depletion of macrophages, collagen deposition decreased compared with control group (Fig. 2C). Collagen volume

fraction was down-regulated from (43.14 ± 8.57)% to (30.73 ± 7.39)%. Differences were statistically significant (P<0.05).

Collagen 1 and 3 in the wound site and marginal area were stained by immunochemistry. Macrophage depletion resulted in substantial attenuation of collagen 1 as well as elevation of collagen 3 compared with those in control group (Fig. 2E and G). The mean densities of abnormal collagens in the wound and margin altered in the absence of macrophages. Administration of clodronate liposome led to an approximately 70% reduction of collagen 1 in the wound and an approximately 30% reduction in the margin (Fig. 2F). Differences were statistically significant (P<0.05). There was about 1.5 to 3.5 times of collagen 3 following macrophage depletion (Fig. 2H). Differences were statistically significant (P<0.05, P<0.01).

3.4 Macrophages induced cellular proliferation in granulation

During macrophage depletion, proliferating cells in granulation apparently decreased, indicating that macrophages induced cellular proliferation during wound healing (Fig. 2K). The number of $Ki67^+$ cells significantly decreased from (114 ± 12) to (67 ± 10) (Fig. 2L). A significant difference in $Ki67^+$ cell amount was defined in clodronate group and control group (P<0.01).

3.5 Polarization of RAW264.7 macrophage to M2 phenotype

In order to investigate how M2 macrophages regulate wound healing, untreated RAW264.7 macrophages (M0) was stimulate with 20 ng/mL IL-4 for 24 hours to generate M2 phenotype. To confirm M2 polarization, we used flow cytometry to measure the ratio of $F4/80^+CD206^+$ M2 macrophages (Fig. 3A). As expected, the proportion was up-regulated from (6.36 ± 3.30)% to (76.33 ± 5.00)% (Fig. 3B). As shown in Fig. 3C, $F4/80^+$ macrophages were unaffected (P>0.05). There was effective change of the ratio of $CD206^+$ macrophages between non-IL-4 group and IL-4 group (P<0.01).

The morphological differences of M2 macrophage polarization were observed (Fig. 3D). Unstimulated RAW264.7 macrophages (M0) in non-IL-4 group were oval and attached cells with cytoplasmic granules. Stimulated RAW264.7 macrophages (M2) in IL-4 group were characterized with more pseudopods and cytoplasmic granules as compared with M0 phenotype. These differences displayed effective M2 polarization for further research.

3.6 Different levels of anti-fibrotic and pro-fibrotic factors in M0 and M2 macrophages

To further characterize M1 and M2 phenotypes, secretory levels of anti-fibrotic and pro-fibrotic factors were examined using ELISA. Anti-fibrotic factors include IL-6 and TNF-α. Pro-fibrotic factors include IL-10, TGF-β1, and CTGF. Concentration of IL-6 derived from M2 macrophage in conditioned medium was up-

regulated as compared with M0 macrophage (Fig. 3E). Lower TNF-α concentration was observed in M2 macrophage (Fig. 3F). Expression of IL-10 derived from M2 macrophage displayed lower level than M0 macrophage (Fig. 3G). Secretory TGF-β1 expressed more abundantly in M2 macrophage conditioned medium than M0 macrophage (Fig. 3H).

CTGF is suggested to be overproduced by M2 macrophage, which promotes fibroblast proliferation, migration, adhesion, and ECM production in hepatic fibrosis[29]. In Fig. 3I, M2 macrophage was distinguished by higher secreted CTGF level. Further detection of CTGF protein level by western blotting confirmed higher CTGF expression in M2 macrophages than M0 macrophages (Fig. 4A). CTGF expression in M2 phenotype was 2.35-fold more abundant than that in M0 phenotype (Fig. 4B).

3.7 M2 macrophages elevated fibroblast proliferation and migration

Fibrosis is mainly completed by dermal fibroblasts during wound healing[3]. As shown in the wound model in *vivo*, macrophage depletion led to abundantly impaired collagen deposition in the wound sites. In order to investigate how M2 macrophages affect fibroblasts, FBS-free conditioned medium of M0 and M2 macrophages was applied on L929 (mouse fibroblasts). Proliferation and migration of L929 were assessed.

As shown in Fig. 4C, CCK8 assay results indicated that higher OD values (450 nm) of fibroblasts were observed in IL-4 group (M2) as compared with non-IL-4 group (M0) at both 24 h and 48 h (P<0.01). Within groups, significant differences were displayed in the non-IL-4 group (M0) between 0 h and 24 h (P<0.05); and IL-4 group (M2) between 0 h and 24 h (P<0.01).

Migration of L929 (fibroblasts) was assessed by cellular wound healing assay (Fig. 4D and E). At 48 h and 96 h, wound healing rates in IL-4 group (M2) were distinguished from those in non-IL-4 group (M0). Within groups, significant differences were displayed in IL-4 group (M2) between 48 h and 96 h (P<0.05). These data indicated that M2 macrophages promoted fibroblast proliferation and migration.

3.8 Blockade of CTGF in M2 macrophages deactivated fibroblast proliferation and migration

To ensure the hypothesis that M2 macrophages activate fibroblast through secreting CTGF, M2 macrophages were transfected with small interfering RNA (siRNA). Administration of three kinds of siCTGF (siCTGF 1, 2, and 3) significantly reduced CTGF expression in M2 macrophages (Fig. 5A). CTGF expression in control siRNA group was approximately 4-fold more abundant than that in siCTGF 1, 2, and 3 group (Fig. 5B). Thus, siCTGF 3 was selected for further research. As shown in Fig. 5C, siCTGF significantly reduced secreted CTGF level at both 24 h and 48 h (P<0.01). Within groups, significant differences were displayed in control siRNA group between 24 h and 48 h (P<0.01); and siCTGF group between 24 h and 48 h (P<0.05).

FBS-free conditioned mediums of macrophages in control siRNA group and siCTGF group were applied on L929 (fibroblasts). Proliferation and migration of L929 were assessed as described above. As shown in Fig. 5D, CCK8 assay results indicated that lower OD values (450 nm) of fibroblasts were observed in siCTGF group as compared with control siRNA group at both 24 h and 48 h (P<0.01). Within groups, there are significant differences in control siRNA group between 0 h and 24 h (P<0.01); and siCTGF group between 0 h and 24 h (P<0.05).

Migration of L929 (fibroblasts) was assessed by cellular wound healing assay (Fig. 5E and F). At 24 h, no significant difference was found between control siRNA group and siCTGF group (P>0.05). At 48 h, wound healing rates in siCTGF group decreased as compared with those in control siRNA group (P<0.05). These results revealed that blockade of CTGF in M2 macrophages deactivated fibroblast proliferation and migration.

3.9 Recombinant CTGF restored fibroblast proliferation and migration

For further confirmation, recombinant CTGF was applied on fibroblasts along with FBS-free conditioned medium of M2 macrophages. As shown in Fig. 6A, CCK8 assay results indicated that down-regulated OD values (450 nm) of fibroblasts were observed in siCTGF group as compared with control siRNA group at both 24 h and 48 h (P<0.01). The OD values up-regulated in siCTGF + CTGF group as compared with siCTGF group at both 24 h and 48 h (P<0.01). Within groups, there are significant differences in siCTGF + CTGF group between 0 h and 24 h (P<0.01); and siCTGF + CTGF group between 24 h and 48 h (P<0.05).

Migration was assessed by cellular wound healing assay (Fig. 6B and C). At 24 h and 48 h, wound healing rates in siCTGF group decreased as compared with those in control siRNA group (P<0.01). Administration of CTGF elevated wound healing rates in siCTGF + CTGF group as compared with siCTGF group (P<0.05). Taken together, recombinant CTGF restored the promotional effects of M2 macrophages on fibroblast proliferation and migration.

3.10 M2 macrophages secreted CTGF to mediate fibroblasts via activating AKT/ERK1/2/STAT3 pathway

CTGF has been reported to be closely related with tissue repair through enhancing phosphorylation of p38, ERK1/2, JNK, and AKT in fibroblasts. We assessed AKT/p-AKT, ERK1/2/p-ERK1/2, and STAT3/p-STAT3 expressions in fibroblasts by western blotting (Fig. 6D and E). Although total AKT, ERK1/2, and STAT3 expressions were not significantly changed among control siRNA group, siCTGF group, and siCTGF + CTGF group, p-AKT, p-ERK1/2, and p-STAT3 were substantially reduced in the absence of CTGF (P<0.01). Complement of CTGF restored p-AKT, p-ERK1/2, and p-STAT3 (P<0.05, P<0.01). Overall, these observations illustrated that M2 macrophages secreted CTGF to mediate fibroblasts via activating ERK1/2/STAT3 and AKT/STAT3 signaling pathway.

4. Discussion

Cutaneous wound healing comprises three successive and overlapping stages, containing inflammation phase, proliferation phase, and tissue remodeling phase. Fibrous repair is believed to be one of the most vital pathophysiological processes during cutaneous wound healing. However, the underlying mechanism is not clear enough. Even though recent studies have attempted to determine that macrophages contribute to all stages of wound and repair, additional evidences are needed to better understand the role of macrophages.

Dramatic phenotypic varieties of macrophages occur when exposing to external stimuli. Macrophages are broadly classified as M1 phenotype and M2 phenotype, depending on distinguished stimuli, surface markers, along with secretory proteins. M1 macrophages are responded to Th1 cytokines, while M2 macrophages are responded by Th2 cytokines[28]. Subtypes of M2-polarized macrophages include M2a, M2b, and M2c[29, 30]. M2a subtype, which is referred to be “alternatively activated macrophage”, is stimulated by IL-4/IL-13 and characterized with markers, including CD206, CD163, and CD209. M2 phenotype is also be called “pro-fibrotic macrophage”. M2 macrophages secrete TGF-beta and CTGF[30]. M2b subtype, which is referred to be “immunoregulatory macrophage”, is stimulated by IL-1, lipopolysaccharide (LPS), and immunoglobulin (IgG) complex. M2b macrophages secrete IL-1, IL-6, IL-12, and TNF-alpha. M2c subtype, which is referred to be “anti-inflammatory macrophage”, is stimulated by IL-10, C-X-C chemokine receptor 3 (CXCRL3), and TGF-beta[31, 32]. M2c macrophages are able to secrete IL-10 and TGF-beta. Moreover, a specific subtype is defined as “fibrolytic macrophage”. These fibrolytic macrophages are able to secrete degradative enzymes, such as matrix metalloproteinase 9 (MMP9) and MMP13.

During cutaneous wound healing, macrophages recruit to wound site mainly from peripheral blood soon after the wound occurs. Large amounts of M1 macrophages infiltrate in the wound area at 1 to 2 days post injury[6]. Most M1 macrophages further polarized to M2 macrophages at 3 days post injury[7]. Fibrosis is a common progression of organ injury and repair, in which M2 macrophages play a central role. Previous researches have shown that M2 macrophages were strongly associated with renal pathogenic fibrosis [33]. Cardiac macrophages isolated from ischemic cardiac fibrosis were characterized with high M2 marker CD206 [34]. In non-healing wounds, mesenchymal stem cells induced their polarization in M2 phenotype, leading to skin repair [35]. M2 macrophages promoted fibrotic activities of human dermal fibroblasts in vitro [36]. In this research, we investigated that M2 macrophages depletion with clodronate liposome at 4, 6, and 8 days post injury delayed wound healing rates. Consistent with this phenomenon, depletion of M2 macrophages significantly slashed the profibrotic effect through inhibiting collagen 1 and collagen 3 deposition at the wound site and the area around the wound.

In this research, we induced M2 polarization in *vitro* and identified that M2 macrophages secreted abundant CTGF. Moreover, M2 macrophages were verified to promote proliferation and migration of L929 fibroblasts via secreting CTGF. Previous studies suggested that CTGF enhanced renal fibrosis through activating ERK1/2 signaling pathway[37, 38]. CTGF promoted human corneal fibroblast proliferation and collagen contraction through stimulating ERK/STAT3 signaling pathway[39]. CTGF was found to be closely related with tissue repair and fibrosis via phosphorylating p38, ERK1/2, JNK, and AKT[40]. In our

research, selective expression of connective tissue growth factor in fibroblasts in *vitro* promotes systemic tissue fibrosis to elevate the phosphorylation of AKT, ERK1/2 and STAT3 in L929 fibroblasts. Inhibition of *CTGF* in M2 macrophages down-regulated p-AKT, p-ERK1/2 and p-STAT3 in L929 fibroblasts, which were possibly related with fibrous repair in cutaneous wound healing.

Taken together, M2 macrophages regulated fibrosis of cutaneous wound healing via secreting CTGF, which further activating AKT, ERK1/2 and STAT3 phosphorylation in L929 fibroblasts. Further studies are necessary to better understand the mechanism.

Declarations

Acknowledgements

We are indebted to all individuals who participated in or helped with this research project.

Author Contributions

All authors participated in the design, interpretation of the studies and analysis of the data and review of the manuscript; **Si-Min Zhang** devoted to study design, data collection, and manuscript preparation. **Chuan-Yuan Wei** and **Qiang Wang** devoted to study design and data interpretation. **Lu Wang** participated in statistical analysis and paper revision. **Lu Lu** participated in statistical analysis and data interpretation. **Fazhi Qi** provided substantial advice in study design, division of labor, manuscript preparation, and funds collection.

Conflict of Interest

None.

References

1. Rockey DC, Bell PD, Hill JA. Fibrosis–a common pathway to organ injury and failure. New Engl J Med 2015;372:1138–1149
2. Martin P, Leibovich SJ. Inflammatory cells during wound repair: the good, the bad and the ugly. Trends Cell Biol 2005;15:599–607
3. Hopkinson-Woolley J, Hughes D, Gordon S et al Macrophage recruitment during limb development and wound healing in the embryonic and foetal mouse. J Cell Sci 1994;107:1159–1167
4. *van* Furth R, Nibbering PH, *van* Dissel JT et al The characterization, origin, and kinetics of skin macrophages during inflammation. J Invest Dermatol 1985;85:398–402
5. Martin P, D'Souza D, Martin J et al Wound healing in the PU.1 null mouse–tissue repair is not dependent on inflammatory cells. Curr Biol 2003;13:1122–1128
6. Tacke F, Randolph GJ. Migratory fate and differentiation of blood monocyte subsets. Immunobiology 2006;211:609–618

7. Ginhoux F, Tacke F, Angeli V. Langerhans cells arise from monocytes in vivo. Nat Immunol 2006;7:265–273
8. Klahr S, Morrissey J. Obstructive nephropathy and renal fibrosis. Am J Physiol Renal Physiol 2002;283:F861–F875
9. Leask A (2013) CCN2: a novel, specific and valid target for anti-fibrotic drug intervention. Expert Opin Ther Targets 17:1067–1071
10. Takigawa M (2018) An early history of CCN2/CTGF research: the road to CCN2 via hcs24, ctgf, ecogenin, and regenerin. J Cell Commun Signal 12:253–264
11. Lau LF (2016) Cell surface receptors for CCN proteins. J Cell Commun Signal 10:121–127
12. Montford JR, Furgeson SB. A new CTGF target in renal fibrosis. Kidney Int 2017;92:784–786
13. Shi C, Li G, Tong Y, Deng Y, *et al.* Role of CTGF gene promoter methylation in the development of hepatic fibrosis. Am J Transl Res 2016;8:125–132
14. Kok HM, Falke LL, Goldschmeding R et al Targeting CTGF, EGF and PDGF pathways to prevent progression of kidney disease. Nat Rev Nephrol 2014;10:700–711
15. Ferdoushi S, Paul D, Ghosh CK et al Correlation of Connective Tissue Growth Factor (CTGF/CCN2) with Hepatic Fibrosis in Chronic Hepatitis B. Mymensingh Med J 2015;24:558–563
16. Makino K, Makino T, Stawski L et al Anti-connective tissue growth factor (CTGF/CCN2) monoclonal antibody attenuates skin fibrosis in mice models of systemic sclerosis. Arthritis Res Ther 2017;19:134
17. Leask A (2017) CCN2 in Skin Fibrosis. Methods Mol Biol 1489:417–421
18. Hayakawa K, Ikeda K, Fujishiro M et al Connective Tissue Growth Factor Neutralization Aggravates the Psoriasis Skin Lesion: The Analysis of Psoriasis Model Mice and Patients. Ann Dermatol 2018;30:47–53
19. Alfaro MP, Deskins DL, Wallus M. A physiological role for connective tissue growth factor in early wound healing. Lab Invest 2013;93:81–95
20. Nakai K, Karita S, Igarashi J et al COA-Cl prevented TGF-beta1-induced CTGF expression by Akt dephosphorylation in normal human dermal fibroblasts, and it attenuated skin fibrosis in mice models of systemic sclerosis. J Dermatol Sci 2019;94:205–212
21. Henrot P, Truchetet ME, Fisher G et al CCN proteins as potential actionable targets in scleroderma. Exp Dermatol 2019;28:11–18
22. Janis JE, Harrison B. Wound Healing: Part I. Basic Science. Plast Reconstr Surg 2016;138:9S–17S
23. Salehi S, Reed EF. The divergent roles of macrophages in solid organ transplantation. Curr Opin Organ Transplant 2015;20:446–453
24. Kamdem SD, Moyou-Somo R, Brombacher F. Host Regulators of Liver Fibrosis During Human Schistosomiasis. Front Immunol 2018;9:2781
25. Ikezumi Y, Suzuki T, Karasawa T et al Identification of alternatively activated macrophages in new-onset paediatric and adult immunoglobulin A nephropathy: potential role in mesangial matrix

expansion. Histopathology 2011;58:198–210

26. Ikezumi Y, Suzuki T, Yamada T et al Alternatively activated macrophages in the pathogenesis of chronic kidney allograft injury. Pediatr Nephrol 2015;30:1007–1017
27. Zhang S, Chen C, Ying J et al Alda-1, an Aldehyde Dehydrogenase 2 Agonist, Improves Cutaneous Wound Healing by Activating Epidermal Keratinocytes via Akt/GSK-3beta/beta-Catenin Pathway. Aesthetic Plast Surg 2020;44:993–1005
28. Smigiel KS, Parks WC. Macrophages, Wound Healing, and Fibrosis: Recent Insights. Curr Rheumatol Rep 2018;20:17
29. Smith TD, Tse MJ, Read EL et al Regulation of macrophage polarization and plasticity by complex activation signals. Integr Biol (Camb) 2016;8:946–955
30. Edholm ES, Rhoo KH, Robert J. Evolutionary Aspects of Macrophages Polarization. Results Probl Cell Differ 2017;62:3–22
31. Salehi S, Reed EF. The divergent roles of macrophages in solid organ transplantation. Curr Opin Organ Transplant 2015;20:446–453
32. Martinez FO, Gordon S. The M1 and M2 paradigm of macrophage activation: time for reassessment. F1000Prime Rep 2014;6:13
33. Tang PM, Nikolic-Paterson DJ, Lan HY. Macrophages: versatile players in renal inflammation and fibrosis. Nat Rev Nephrol 2019;15:144–158
34. Carlson S, Helterline D, Asbe L et al Cardiac macrophages adopt profibrotic/M2 phenotype in infarcted hearts: Role of urokinase plasminogen activator. J Mol Cell Cardiol 2017;108:42–49
35. Harrell CR, Markovic BS, Fellabaum C et al The role of Interleukin 1 receptor antagonist in mesenchymal stem cell-based tissue repair and regeneration. Biofactors 2020;46:263–275
36. Zhu Z, Ding J, Ma Z et al Alternatively activated macrophages derived from THP-1 cells promote the fibrogenic activities of human dermal fibroblasts. Wound Repair Regen 2017;25:377–388
37. Liu XC, Liu BC, Zhang XL et al Role of ERK1/2 and PI3-K in the regulation of CTGF-induced ILK expression in HK-2 cells. Clin Chim Acta 2007;382: 89–94
38. Yang M, Huang H, Li J et al Connective tissue growth factor increases matrix metalloproteinase-2 and suppresses tissue inhibitor of matrix metalloproteinase-2 production by cultured renal interstitial fibroblasts. Wound Repair Regen 2007;15:817–824
39. Radhakrishnan SS, Blalock TD, Robinson PM et al Effect of connective tissue growth factor on protein kinase expression and activity in human corneal fibroblasts. Invest Ophthalmol Vis Sci 2012;53:8076–8085
40. Sonnylal S, Xu SW, Leoni P et al Selective expression of connective tissue growth factor in fibroblasts in vivo promotes systemic tissue fibrosis. Arthritis Rheum 2010;62:1523–1532

Figures

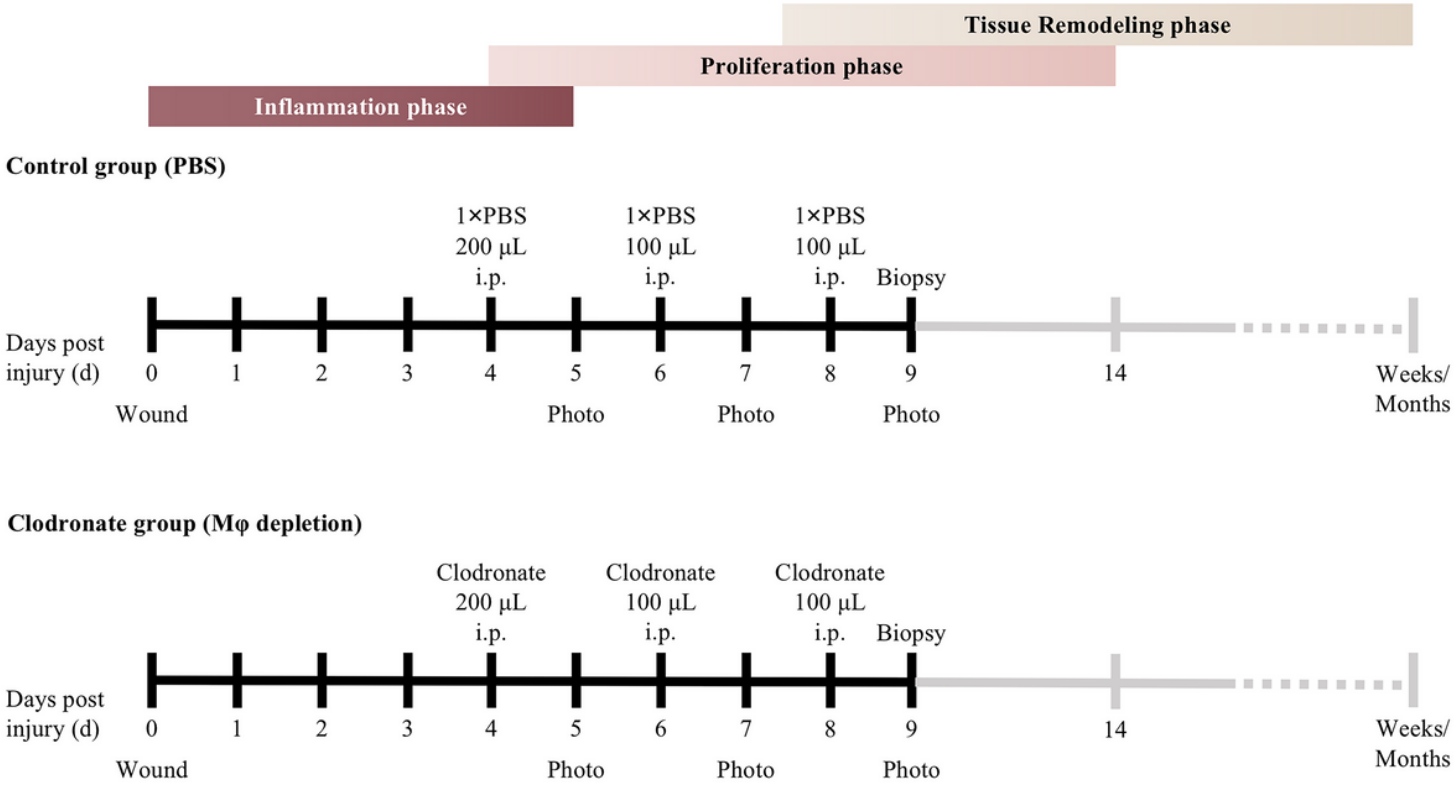

Figure 1

Schematic representation of macrophage depletion by clodronate liposome in cutaneous wound healing. The wound model was established at 0-day post injury (dpi). Mice were injected (i.p.) with PBS or clodronate liposome at 4, 6, and 8 dpi. The wound healing rates were estimated according to the wound photos at 0, 5, 7, and 9 dpi. The wound tissues were collected at 9 dpi for further analysis.

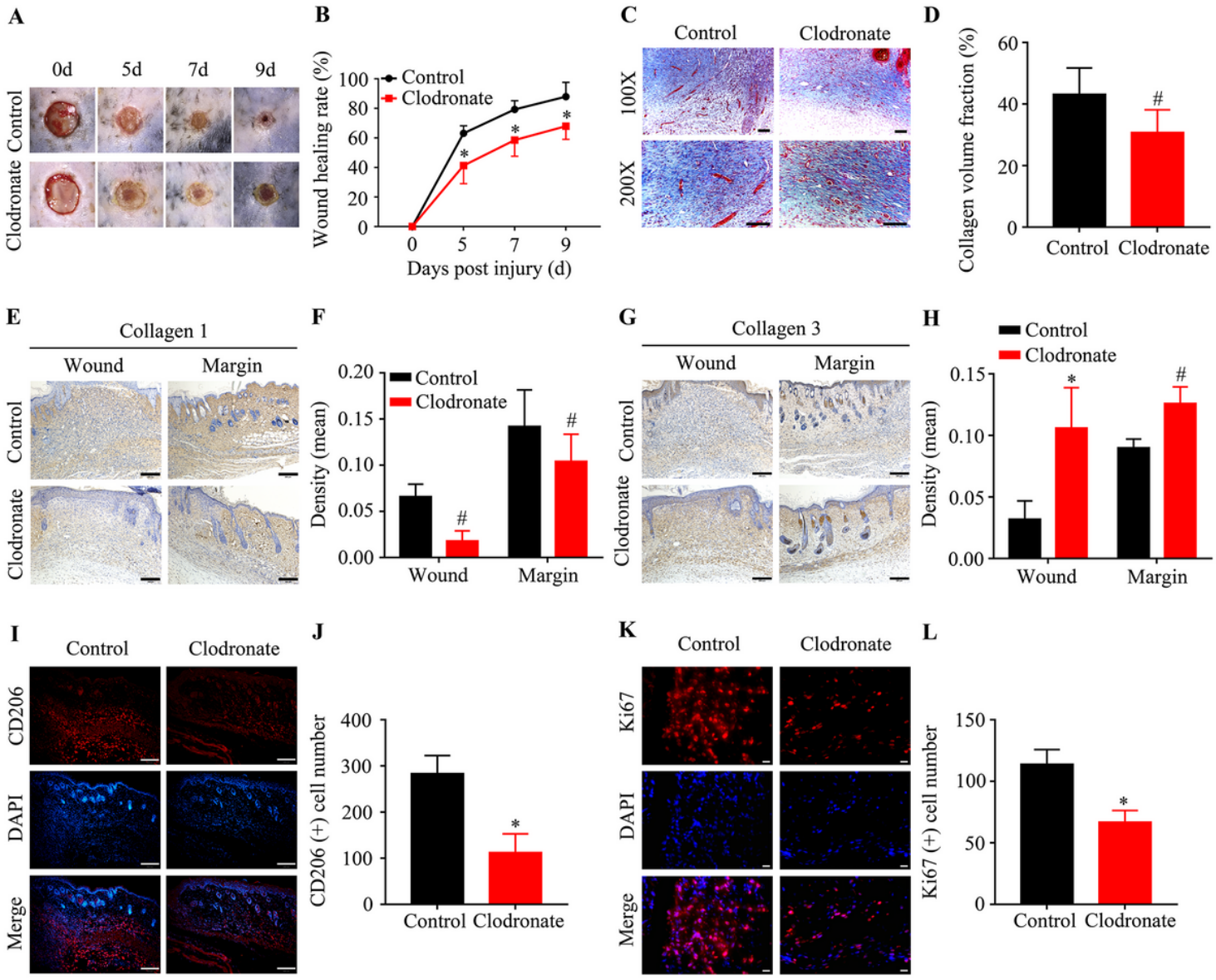

Figure 2

Macrophage depletion during wound healing impaired wound closure, granulation formation, collagen deposition, and proliferation. (A) Macroscopic appearance of wound areas in control group (PBS) and macrophage depletion group (clodronate liposome) at 0, 5, 7, and 9 dpi (5 mice for each time point). (B) The wound sizes were determined by ImageJ software and represented as wound healing rates. (C) Masson's trichrome staining of the wound sites were performed at 9 dpi (n=5). Scale bar represents 100 μm. (D) The collagen volume fraction was assessed by ImageJ software. (E) Collagen 1 at 9 dpi was stained brown by immunochemistry (n=5). Scale bar represents 200 μm. (F) The mean density of collagen 1 was calculated by Image-Pro Plus 6.0. (G) Collagen 3 at 9 dpi was stained brown by immunochemistry (n=5). Scale bar represents 200 μm. (H) The mean density of collagen 3 was estimated by Image-Pro Plus 6.0 software. (I) CD206+ M2 macrophages at 9 dpi were stained red by immunofluroscence (n=5). Scale bar represents 200 μm. (J) Morphometric CD206+ M2 macrophages was quantified by ImageJ software. (K) Ki67+ cells in granulation were stained red by

immunofluroscence. Scale bar represents 20 μm. (L) Morphometric Ki67+ cells was quantified by ImageJ. Values were represented as mean±SD. # P<0.05, * P<0.01.

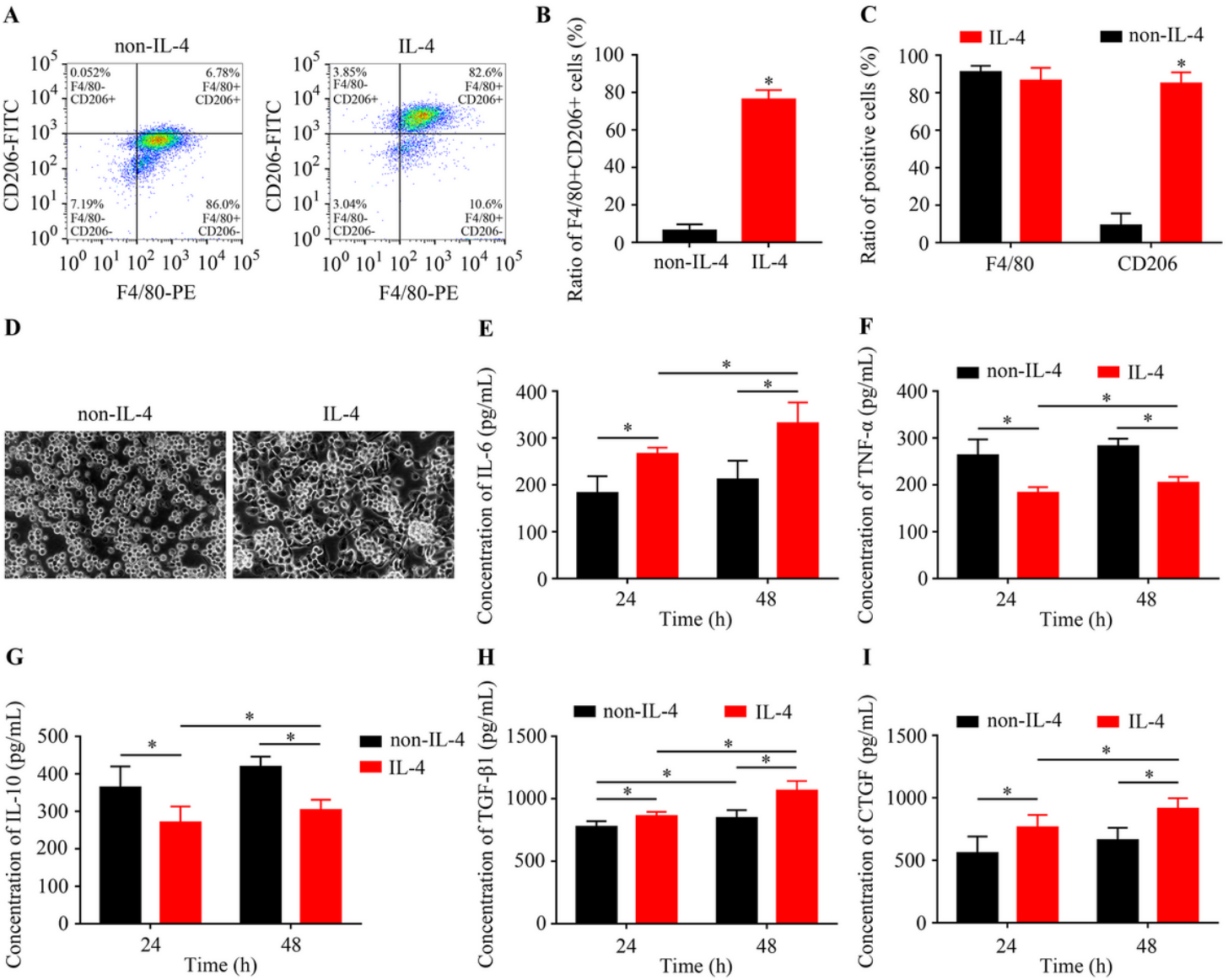

Figure 3

Polarization of RAW264.7 macrophage to M2 phenotype. (A) Polarized RAW264.7 macrophages by IL-4 stimulation were marked using F4/80 and CD206 by flow cytometry. (B) Ratio of F4/80+CD206+ macrophages after IL-4 stimulation were assessed. (C) Ratio of F4/80+ macrophages and CD206+ macrophages after IL-4 stimulation were separately counted. (D) Morphologic charateristics of macrophages in non-IL-4 group (M0) and IL-4 group (M2) were observed. (E) Concentration of IL-6 in FBS-free conditioned medium of M0 and M2 macrophages were assessed at 24 h and 48 h by ELISA. (F) Concentration of TNF-α in FBS-free conditioned medium of M0 and M2 macrophages were detected at 24 h and 48 h by ELISA. (G) Concentration of IL-10 in FBS-free conditioned medium of M0 and M2 macrophages were analyzed at 24 h and 48 h by ELISA. (H) Concentration of TGF-β1 in FBS-free conditioned medium of M0 and M2 macrophages were assessed at 24 h and 48 h by ELISA. (I)

Concentration of CTGF in FBS-free conditioned medium of M0 and M2 macrophages were detected at 24 h and 48 h by ELISA. Values were represented as mean±SD. * P0.01.

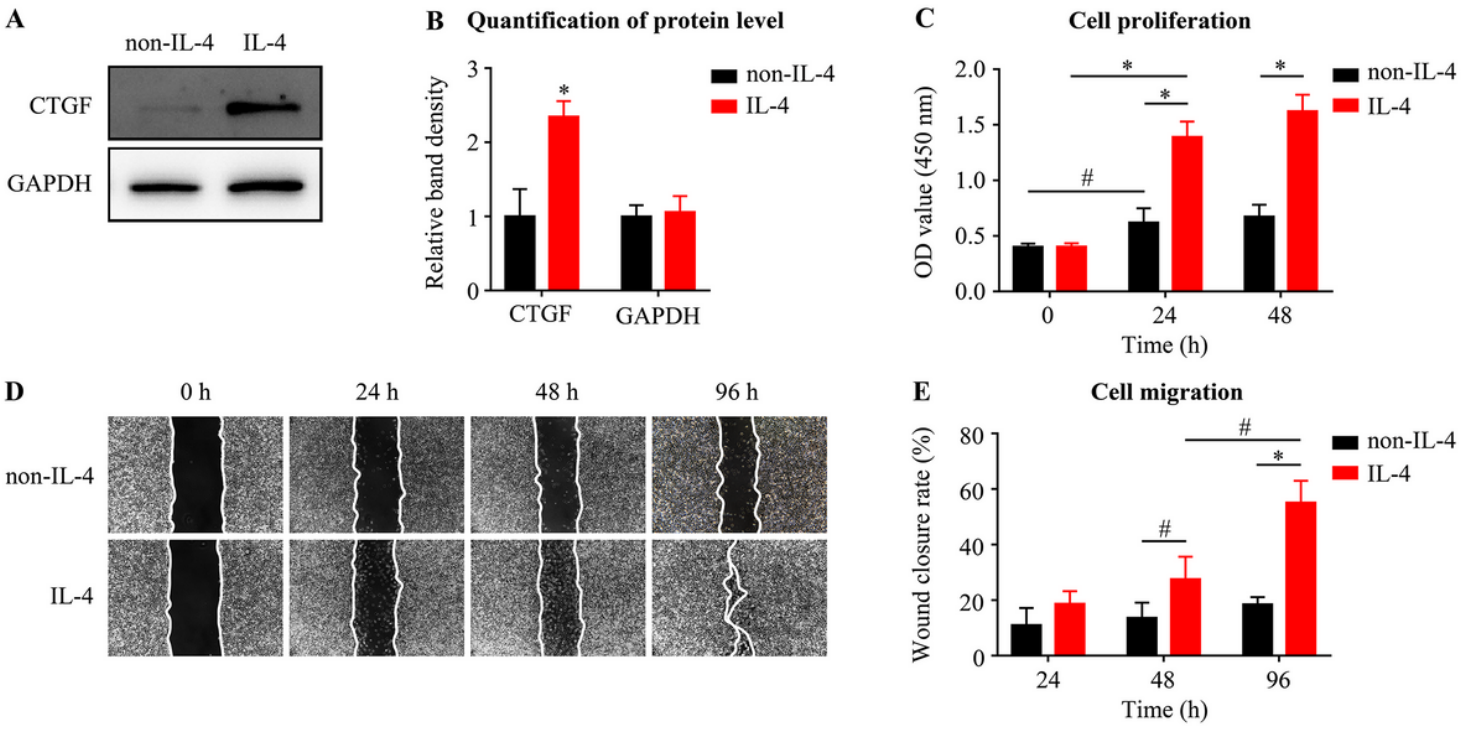

Figure 4

M2 macrophages elevated fibroblast proliferation and migration. (A) CTGF expressions of macrophages in non-IL-4 group (M0) and IL-4 group (M2) were detected by western blotting. (B) The relative band densities of CTGF and GAPDH were assessed by ImageJ software. (C) After administration of FBS-free conditioned medium of M0 and M2 macrophages on L929, OD values at 450 nm were assessed at 0, 24, and 48 h by CCK8 assay. (D) After administrating FBS-free conditioned medium of M0 and M2 macrophages on L929, L929 migration was detected at 0, 24, 48, and 96 h. (E) Wound closure rates were calculated. Values were represented as mean±SD. # P0.05, * P0.01.

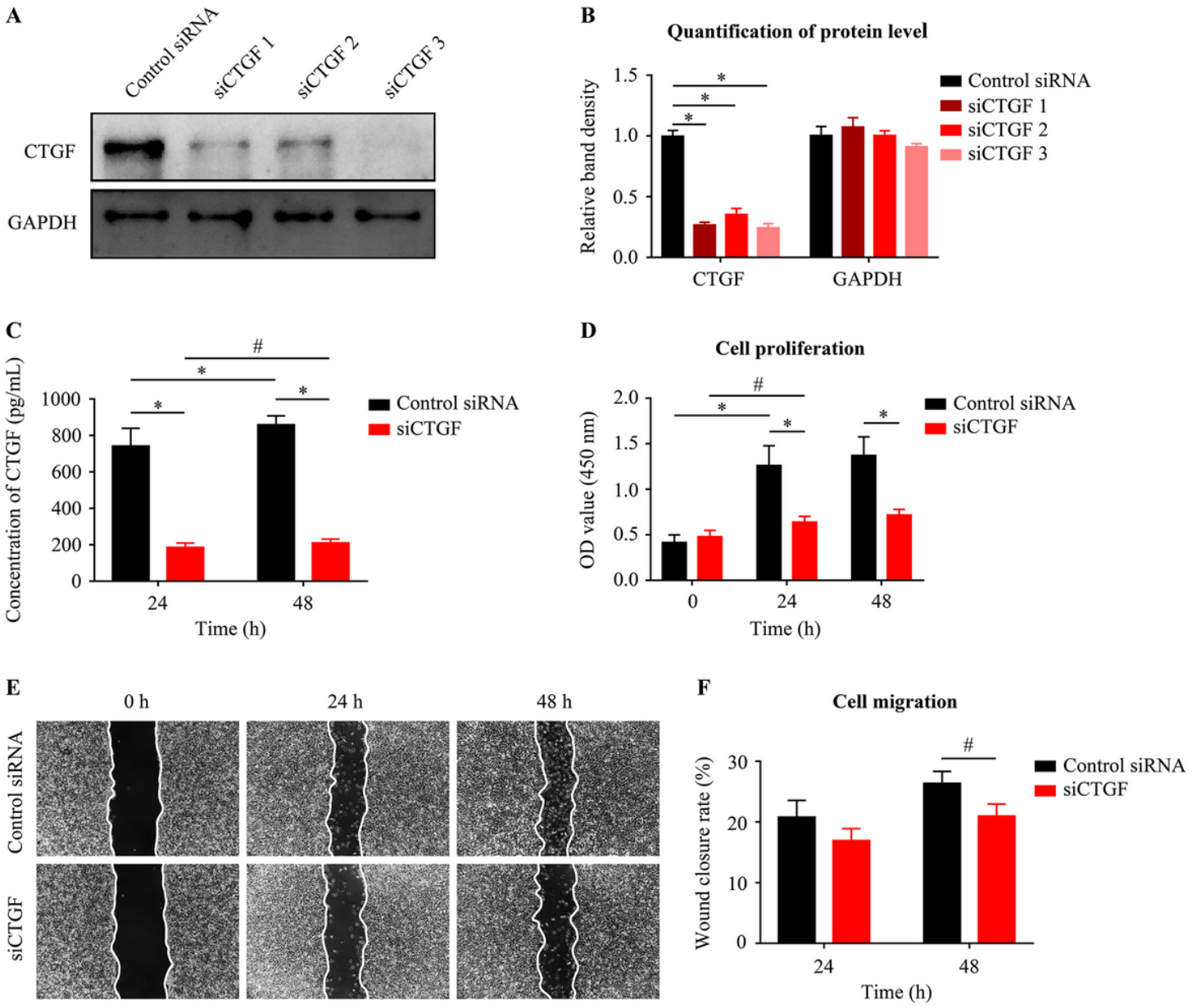

Figure 5

Blockade of CTGF in M2 macrophages deactivated fibroblast proliferation and migration. (A) Protein levels CTGF in M2 macrophages after administration of siCTGF 1, siCTGF 2, and siCTGF 3. (B) The relative band densities of CTGF and GAPDH were assessed by ImageJ software. (C) After administration of siCTGF on M2 macrophages, concentration of CTGF in FBS-free conditioned medium was analyzed at 24 h and 48 h by ELISA. (D) After administrating FBS-free conditioned medium of M2 macrophages in control siRNA group and siCTGF group, OD values at 450 nm were assessed at 0, 24, and 48 h by CCK8 assay. (E) After administrating FBS-free conditioned medium of M2 macrophages in control siRNA group and siCTGF group, L929 migration was detected at 0, 24, 48 h. (F) Wound closure rates were calculated. The values were represented as mean±SD. # P□0.05, * P□0.01.

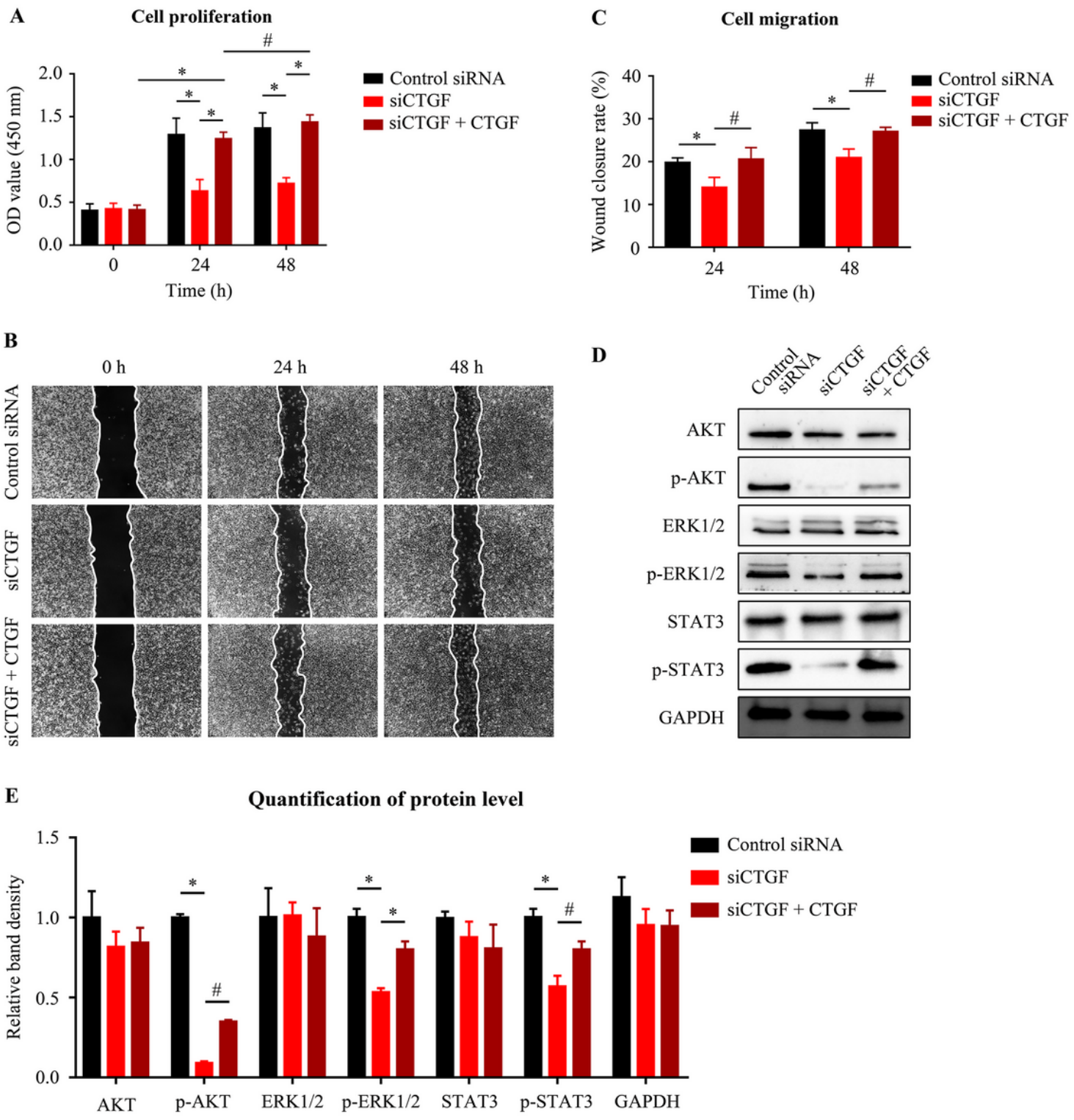

Figure 6

Recombinant CTGF restored fibroblast proliferation and migration via activating AKT/ERK1/2/STAT3 pathway. (A) Recombinant CTGF was applied on fibroblasts along with FBS-free conditioned medium of M2 macrophages. OD values at 450 nm were assessed at 0, 24, and 48 h by CCK8 assay. (B) After administrating FBS-free conditioned medium of M2 macrophages in control siRNA group, siCTGF group, and siCTGF + CTGF group, L929 migration was assessed at 0, 24, and 48 h by CCK8 assay. (C) Wound

closure rates were calculated. (D) AKT/p-AKT, ERK1/2/p-ERK1/2, and STAT3/p-STAT3 expressions in fibroblasts were assessed by western blotting. (E) Relative band densities of CTGF and GAPDH were assessed by ImageJ. Values were represented as mean±SD. # P0.05, * P0.01.

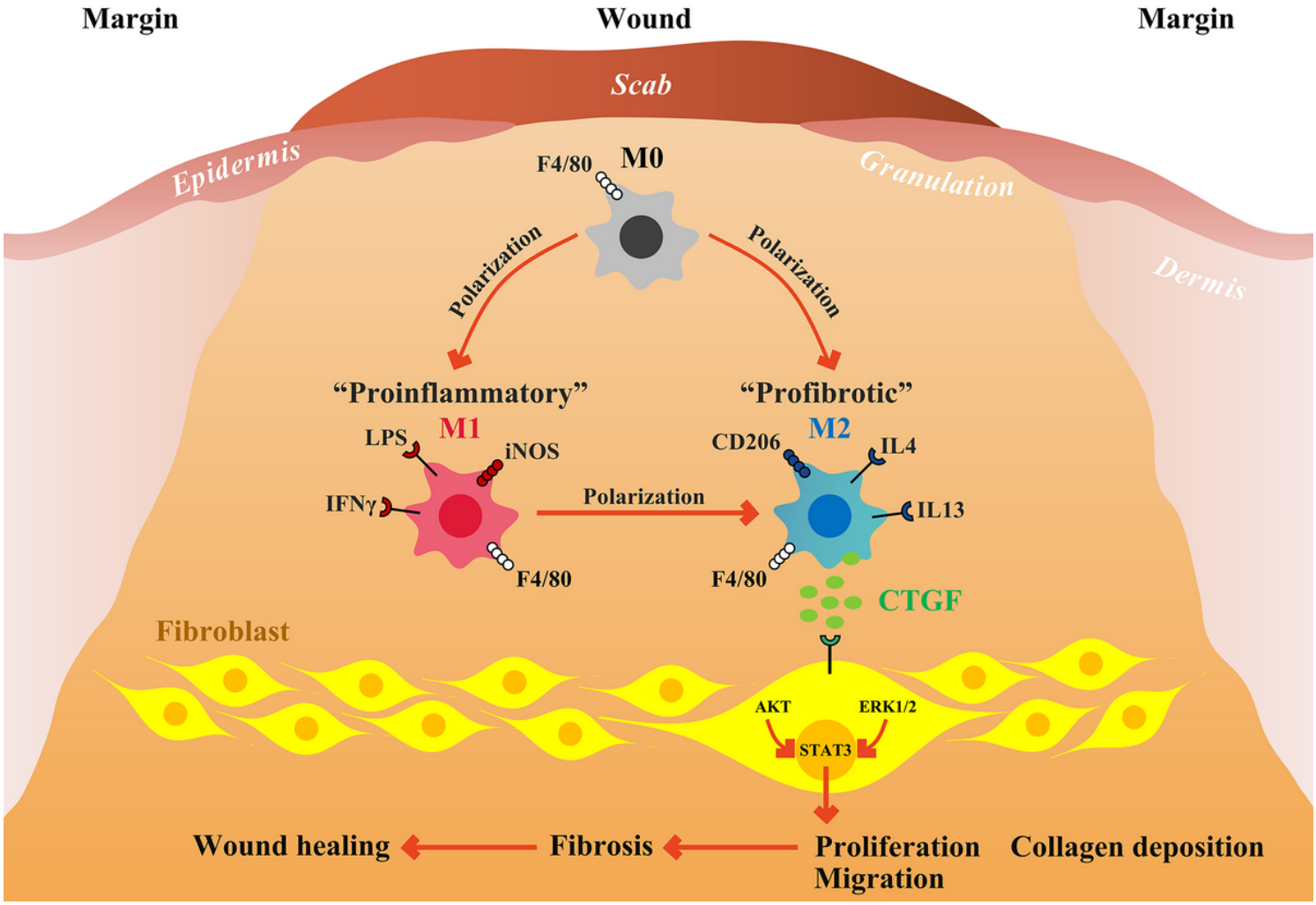

Figure 7

Schematic representation: M2 macrophages secreted CTGF to mediate fibroblasts via activating AKT/ERK1/2/STAT3 pathway in cutaneous wound healing. In cutaneous wound healing, "profibrotic" M2 macrophages mainly participate in fibrosis. F4/80+CD206+ M2 macrophages can be polarized from F4/80+ M0 and F4/80+iNOS+ "proinflammatory" M1. Polarization of M1 macrophages is classically induced by LPS and IFN-γ. Polarization of M2 macrophages is classically stimulated by IL-4/IL-13. M2 regulates fibroblasts via secreting CTGF. CTGF further activates AKT/STAT3 and ERK1/2/STAT3 signaling pathway in fibroblasts, thus improving cell proliferation, migration, and collagen deposition. Our research suggested a prominent role of M2 macrophages in cutaneous wound healing and possible mechanism.